HHS Public Access

Author manuscript

J Bone Miner Res. Author manuscript; available in PMC 2015 June 06.

Published in final edited form as:

J Bone Miner Res. 2014 August ; 29(8): 1872–1885. doi:10.1002/jbmr.2213.

A Novel Osteogenic Oxysterol Compound for Therapeutic Development to Promote Bone Growth: Activation of Hedgehog Signaling and Osteogenesis through Smoothened Binding

Scott R. Montgomery[1], **Taya Nargizyan**[2], **Vicente Meliton**[2], **Sigrid Nachtergaele**[3], **Rajat Rohatgi**[4], **Frank Stappenbeck**[2], **Michael E. Jung**[5], **Jared S. Johnson**[1], **Bayan Aghdasi**[1], **Haijun Tian**[1], **Gil Weintraub**[1], **Hirokazu Inoue**[1], **Elisa Atti**[6], **Sotirios Tetradis**[6], **Renata C Pereira**[7], **Akishige Hokugo**[8], **Raed Alobaidaan**[1], **Yanlin Tan**[1], **Theodor J. Hahn**[9], **Jeffrey C Wang**[10], and **Farhad Parhami**[2,*]

[1]Department of Orthopedic Surgery, UCLA, Los Angeles, California

[2]Department of Medicine, David Geffen School of Medicine, UCLA, Los Angeles, California

[3]Department of Biochemistry, Stanford University School of Medicine, Stanford, California

[4]Department of Medicine, Stanford University School of Medicine, Stanford, California

[5]Department of Chemistry and Biochemistry, UCLA, Los Angeles, California

[6]School of Dentistry, UCLA, Los Angeles, California

[7]Department of Pediatric Nephrology, UCLA, Los Angeles, California

[8]Department of Plastic Surgery, UCLA, Los Angeles, California

[9]VA Greater Los Angeles Healthcare System and Geriatric Research, Education, and Clinical Center, Los Angeles, California

[10]Department of Orthopedic Surgery, USC, Los Angeles, California

Abstract

Osteogenic factors are often used in orthopedics to promote bone growth, improve fracture healing, and induce spine fusion. Osteogenic oxysterols are naturally occurring molecules that were shown to induce osteogenic differentiation *in vitro* and promote spine fusion *in vivo*. The purpose of this study was to identify an osteogenic oxysterol more suitable for clinical development than those previously reported, and evaluate its ability to promote osteogenesis *in vitro* and spine fusion in rats *in vivo*. Among more than 100 oxysterol analogues synthesized, Oxy133 induced significant expression of osteogenic markers Runx2, osterix (OSX), alkaline phosphatase (ALP), bone sialoprotein (BSP), and osteocalcin (OCN) in C3H10T1/2 mouse embryonic fibroblasts and in M2-10B4 mouse marrow stromal cells. Oxy133-induced activation

*Corresponding Author: Farhad Parhami, Ph.D., M.B.A., Professor of Medicine, David Geffen School of Medicine at UCLA, Center for the Health Sciences, A2-237, 10833 Le Conte Avenue, Los Angeles, CA. 90095, Tel: 310-825-5729, fparhami@mednet.ucla.edu.

Disclosure– Drs. Parhami and Jung disclose that they are founders of MAX BioPharma Inc., which has licensed the rights to Oxy133 from UCLA, and that they have financial interests in the technology presented here. Dr. Theodore Hahn also discloses having financial interests in MAX BioPharma. In addition, as part of the licensing agreement, UCLA holds equity in MAX BioPharma.

All other authors state that they have no conflicts of interest.

of an 8×-Gli luciferase reporter, its direct binding to Smoothened, and the inhibition of Oxy133-induced osteogenic effects by the Hedgehog (Hh) pathway inhibitor, cyclopamine, demonstrated the role of Hh pathway in mediating osteogenic responses to Oxy133. Oxy133 did not stimulate osteogenesis via BMP or Wnt signaling. Oxy133 induced the expression of OSX, BSP, and OCN and stimulated robust mineralization in primary human mesenchymal stem cells. *In vivo*, bilateral spine fusion occurred through endochondral ossification and was observed in animals treated with Oxy133 at the fusion site on xray after 4 weeks and confirmed with manual assessment, micro CT (μCT), and histology after 8 weeks, with equal efficiency to recombinant human bone morphogenetic protein-2 (rhBMP-2). Unlike rhBMP-2, Oxy133 did not induce adipogenesis in the fusion mass and resulted in denser bone evidenced by greater BV/TV ratio and smaller trabecular separation. Findings here suggest that Oxy133 has significant potential as an osteogenic molecule with greater ease of synthesis and improved time to fusion compared to previously studied oxysterols. Small molecule osteogenic oxysterols may serve as the next generation of bone anabolic agents for therapeutic development.

Keywords

oxysterol; spinal fusion; BMP2; osteogenesis; adipogenesis

Introduction

Despite the endless number of medical scenarios requiring bone formation, such as fracture healing, spine fusion, and osteoporosis, there is currently no safe and cost-effective osteogenic factor to promote bone formation (1–4). Spine fusion is often performed by orthopedic surgeons and neurosurgeons alike to address degenerative disc disease and arthritis affecting the lumbar and cervical spine. Historically, autogenous bone graft, commonly taken from the iliac crest of the patient, has been used to augment fusion between vertebral levels. However, the associated donor site morbidity, increased operating time, and increased blood loss associated with harvesting autogenous bone graft (5–7) has provided incentive to find a safe and effective alternative.

Recombinant human bone morphogenetic-2 (rhBMP-2) is commonly used to promote spine fusion in humans. Its use was approved in 2002 by the US Food and Drug Administration (FDA) for single-level anterior lumbar interbody fusion (8). The use of rhBMP-2 has increased significantly since this time and indications for its use have expanded to include posterior lumbar spinal fusion as well cervical spine fusion. Despite the efficacy of rhBMP-2, recent reports have called into question its safety when employed during spine fusion surgery. Reported complications have included seroma formation, soft tissue swelling, vertebral osteolysis, ectopic bone formation, retrograde ejaculation, and carcinogenicity (9–12). Moreover, airway edema has been observed with its use in the cervical spine, prompting the FDA to issue a Public Health Notification warning for its use in cervical spine operations. To date, no suitable alternative has been identified that would have similar efficacy in inducing fusion without the adverse effects of rhBMP-2 (12).

We previously reported that specific naturally occurring oxysterols have robust osteogenic properties (13). Oxysterols form a large family of oxygenated derivatives of cholesterol that are present in the circulation and in human and animal tissues. These compounds may be formed either by auto-oxidation, as a secondary byproduct of lipid peroxidation, or by the action of specific monooxygenases, most of which are members of the cytochrome P450 family of enzymes. In addition, oxysterols may be derived from dietary intake. The most potent osteogenic naturally occurring oxysterol, 20(*S*)-hydroxycholesterol (20S) (14), is both osteogenic and anti-adipogenic when applied to multipotent MSCs capable of differentiating into osteoblasts and adipocytes. Structural modifications of 20S were previously performed to synthesize more potent analogues of 20S including Oxy34 and Oxy49, which were shown to induce the osteogenic and inhibit the adipogenic differentiation of multipotent bone marrow stromal cells through activation of Hedgehog (Hh) signaling (15). Additionally, Oxy34 and Oxy49 stimulate spine fusion *in vivo* in a rat model of posterolateral spine fusion (15). Despite the great promise that these molecules have shown thus far, both in terms of efficacy and significantly lower production cost as compared with rhBMP-2, improving the potency, ease of synthesis, and cost of these factors would make them a more feasible clinical option for physicians treating long bone fractures, spine disorders, and perhaps even osteoporosis. Moreover, the mechanism of bone formation and properties of bone formed by oxysterols are not well established.

The purpose of this study was to: (1) design an osteogenic oxysterol analogue that would have improved properties to Oxy34 and Oxy49 for further therapeutic development, first in terms of ease of synthesis for scaling up that would also result in lower cost, and second in terms of potency if possible, (2) to evaluate its potential use in clinical scenarios requiring the promotion of bone formation, and (3) to further elucidate the mechanism of action of osteogenic oxysterols and the microstructural properties of bone induced by oxysterols. To this end, structure activity relationship studies were used to identify a novel oxysterol analogue, Oxy133, with greater potency and ease of synthesis than those previously identified. We subsequently aimed to characterize the osteogenic potential of Oxy133 *in vitro* when applied to human MSCs, identify the molecular mechanism by which Oxy133 activates Hh signaling, and evaluate the potential of Oxy133 to promote spine fusion in a rat model *in vivo*.

Materials and Methods

Cell Culture and Reagents

Mouse multipotent bone marrow stromal cell line, M2-10B4 (M2), and embryonic fibroblast cell line C3H10T1/2 (C3H) were purchased from American Type Culture Collection (Rockville, MD) and cultured as we have previously reported (14,15). Treatment to induce osteogenic differentiation was performed in RPMI for M2 cells or DMEM for C3H cells containing 5% fetal bovine serum (FBS), 50μg/ml ascorbate, and 3mM β-glycerophosphate (βGP) (differentiation media). Adipogenic differentiation of C3H cells was induced by treatment of cells with DMEM containing 10% FBS and 10 μM PPARγ activator, Troglitazone (Tro). Chondrogenic differentiation of C3H cells was achieved using a modification of a previously reported pellet culture (36). Briefly, 1 million cells were

pelleted by centrifugation and cultured in DMEM containing 10% FBS and 50 μg/ml ascorbate. In all in vitro experiments, control condition consists of differentiation media without the test agents. Cyclopamine was purchased from EMD Biosciences, Inc. (La Jolla, CA), Tro and Smoothened agonist SAG from Cayman Chemical (Ann Arbor, MI), and rhBMP-2 rmShh, rmTGFβ3, noggin and Dkk-1 from R&D Systems (Minneapolis, MN). Primary human MSCs were purchased from Lonza (Walkersville, MD) and cultured and passaged in growth medium from StemCell Technologies (Vancouver, Canada) according to manufacturer's instructions. Osteogenic differentiation of human MSCs was induced by treating the cells in DMEM low glucose containing antibiotics and 10% heat-inactivated FBS, 10^{-8} M dexamethasone, 10 mM βGP, and 0.2 mM ascorbate.

Alkaline Phosphatase Activity, Oil red O and Von Kossa Staining

Alkaline phosphatase (ALP) activity assay on whole cell extracts (13,14), and von Kossa staining of cell monolayers for mineralization (17) were performed as previously described.

Quantitative RT-PCR

Total RNA was extracted with the RNA isolation Trizol reagent from Ambion, Inc. (Austin, TX) according to the manufacturer's instructions. RNA (1 μg) was reverse-transcribed using reverse transcriptase from Bio-Rad (Hercules, CA) to make single stranded cDNA. Q-RT-PCR reactions were performed using iQ SYBR Green Supermix and an iCycler RT-PCR Detection System (Bio-Rad). Primer sequences for all mouse genes Gli-1, Patched1 (Ptch1), bone-liver-kidney isozyme of alkaline phosphatase (ALP), bone sialoprotein (BSP), Runx2, osterix (OSX), osteocalcin (OCN), collagen 10, aggrecan, PPARγ, aP2 and GAPDH were used as previously described (14) and reported in Supplement Table 1. Human primer sequences for GAPDH, BSP, OSX, and OCN are also reported in Supplemental Table 1. Relative expression levels were calculated using the $2^{\Delta\Delta C}$T method as previously described (15).

Transient Transfection and Gli-Dependent Reporter Assay

Cells at 70% confluence in 24-well plates were transiently transfected with Gli-dependent firefly luciferase and Renilla luciferase vectors as we have previously described (18,19). FuGENE 6 transfection reagent (Roche Applied Science, Indianapolis, IN) was used at a ratio of 3:1 with nuclease-free water and total DNA per well did not exceed 500 ng. Luciferase activity was assessed using the Dual Luciferase Reporter Assay System (Promega Corporation, Madison, WI) according to manufacturer's instructions after cells were treated for 48 hours.

Synthesis and Molecular Characterization of Oxy133

Materials were obtained from commercial suppliers and were used without further purification. Air or moisture sensitive reactions were conducted under argon atmosphere using oven-dried glassware and standard syringe/septa techniques. The reactions were monitored on silica gel TLC plates under UV light (254 nm) followed by visualization with Hanessian's staining solution. Column chromatography was performed on silica gel 60. ^{1}H NMR spectra were measured in $CDCl_3$. Data obtained are reported as follows in ppm from

an internal standard (TMS, 0.0 ppm): chemical shift (multiplicity, integration, coupling constant in Hz.). Stepwise detailed description of the synthesis protocol and characterization of the intermediates and final products, as well as criteria for selection of Oxy133 vs. Oxy34 and Oxy49 are provided in Supplemental Material.

Smoothened Binding Assay

Interaction of oxysterol with Smoothened (Smo) was examined as we previously reported (20). *Smo*-/-:YFP-Smo cells (21) were lysed in hypotonic SEAT buffer (250 mM sucrose, 1 mM EDTA, 10 mM acetic acid, 10 mM triethanolamine, 10 mg/mL leupeptin-pepstatin-chymostatin (LPC) protease inhibitor mix and the SigmaFast EDTA-Free protease cocktail). After removal of nuclei by centrifugation (500×*g*, 5 min), membranes were pelleted by centrifugation at 95,000×*g* for 30 min. Membranes were extracted in an n-dodecyl-b-D-maltopyranoside (DDM) extraction buffer (50 mM Tris pH 7.4, 500 mM NaCl, 10% v/v glycerol, 0.1% w/v DDM and the SigmaFast EDTA-Free protease cocktail) for 4 hours at 4°C, followed by removal of insoluble material by centrifugation (100,000×*g*, 30 min). This membrane extract was incubated with 50uM free 20(S) or Oxy133 or Oxy16 (an oxysterol analogue that does not activate Hh signaling; Parhami et al. unpublished observations) for one hour at 4°C prior to the addition of magnetic beads coupled to *nat*-20(S)-yne or control magnetic beads (20). Binding reactions were incubated overnight at 4°C. In all experiments, the amount of solvent was carefully equalized in each sample. After extensive washing, proteins captured on the beads were eluted with reducing SDS sample buffer. The presence of YFP-Smo in these eluates was determined by quantitative immunoblotting with an anti-GFP antibody (Novus, NB600-308, 1:5000) and infrared imaging (Li-Cor Odyssey system).

Animals

Fifty four 8-week-old male Lewis rats were purchased from Charles River Laboratories (Wilmington, MA) and were maintained and housed at the UCLA vivarium in accordance with regulations set forth by the UCLA Office of Protection of Research Subjects. The study was performed under a protocol approved by the UCLA Animal Research Committee (ARC). Thirty eight animals were used to assess spine fusion and were euthanized using a standard CO_2 chamber 8 weeks after the spinal fusion procedure, and their spines were excised and stored in 40% ethyl alcohol. An additional 16 rats were used in a time course study to evaluate the induction of bone formation via endochondral ossification. Two rats in each group (Oxy133 and rhBMP-2) were sacrificed at 1, 2, 4 and 8 weeks, their vertebrae excised and subjected to histological analysis.

Surgical Procedures

Animals were pre-medicated with sustained release buprenorphine thirty minutes prior to surgery and anesthetized with 2% isoflurane administered in oxygen (1L/min). Posterolateral intertransverse process spinal fusion at L4–L5 was performed as in prior studies (22,23). A 4-cm longitudinal midline incision was made through the skin and subcutaneous tissue over L4–L5 down to the lumbodorsal fascia. A 2-cm longitudinal paramedial incision was then made in the paraspinal muscles bilaterally to expose the transverse processes of L4–L5, which were decorticated with a high-speed burr. The

surgical site was then irrigated with sterile saline, and 5mm×5mm×13mm pieces of absorbable collagen sponge (ACS) (Helistat, Integra Life Sciences) containing dimethyl sulfoxide (DMSO) control (since Oxy133 was dissolved in DMSO), rhBMP-2, or Oxy133 were placed bilaterally, with each implant spanning the transverse processes. The ACS was used to deliver the compounds by soaking the ACS with the aliquots of DMSO, rhBMP-2, or Oxy133 before applying the sponge to the intertransverse process space. The ACS is made of collagen derived from bovine Achilles tendon. The method of application used in this study is identical to what is used in spine surgery in humans, in which rhBMP-2 is mixed with sterile water and soaked with the absorbable collagen sponge prior to implantation. The implants were then covered with the overlying paraspinal muscles and the lumbodorsal fascia and skin were closed with 4–0 Prolene sutures (Ethicon, Inc., Somerville, NJ).

Radiographic Analysis

Posteroanterior radiographs of the lumbar spine were taken on each animal at 4, 6, and 8 weeks after surgery using a Faxitron LX60 cabinet radiography system and evaluated blindly by two independent observers employing the following standardized scale: 0, no fusion; 1, unilateral fusion; and 2, complete bilateral fusion. The scores from the observers were added together and only a score of 4 was considered as complete fusion.

Manual Assessment of Fusion

Eight weeks after surgery, animals were euthanized and the spines were surgically removed and evaluated by two blinded independent observers for motion between levels. Nonunion was recorded if motion was observed between the facets or transverse processes on either side. Complete fusion was recorded if no motion was observed bilaterally. Spines were scored as either fused or not fused. Unanimous agreement was required to consider complete fusion.

μCT

Each excised spine was analyzed by high resolution μCT, using a SkyScan 1172 scanner (SkyScan, Belgium) with a voxel isotropic resolution of 20μm and an X-ray energy of 55kVp and 181mA to further assess the fusion rate and observe the fusion mass as we have previously reported (15). A total of 360 projections were acquired over an angular range of 180° with steps of 0.5 with an exposure time of 220 msec/slice. Five frames were averaged at each rotation step to get better signal to noise ratio. A 0.5 mm aluminum filter was used to narrow down the X-ray beam frequency in order to minimize beam hardening artifact. Virtual image slices were reconstructed using the cone-beam reconstruction software version 2.6 based on the Feldkamp algorithm (SkyScan). These settings produced serial cross-sectional 1024×1024 pixel images. Sample re-orientation and 2D visualization were performed using DataViewer (SkyScan). 3D visualization was performed using Dolphin Imaging version 11 (Dolphin Imaging & Management Solutions, Chatsworth, CA). Fusion was defined as the bilateral presence of bridging bone between the L4 and L5 transverse processes. The reconstructed images were judged to be fused or not fused by two experienced independent observers. To quantify the density of bone formed within each fusion mass, the tissue volume of the mass (TV), trabecular bone volume within the mass

(BV), BV/TV ratio, trabecular thickness, and trabecular separation were calculated. This was performed using DataViewer software with measurements across 501 axial slices (20um per slice, 10.02 mm length) within each fusion mass, centered at the level of the intervertebral body of L4-5.

Histology

After undergoing μCT, two representative specimens from each surgical group were processed undecalcified by dehydration, clearing in xylene and embedding in methyl methacrylate as we have previously reported (15,24). Serial coronal sections were cut with a thickness of 5 μm and stained with toluidine blue pH 6.4. Photomicrographs of sections were obtained as previously reported using a ScanScope XT System (Aperio Technologies, Inc., Vista, CA) at a magnification of 10× in Figure 7A and 20× in Figure 7B (25). Rat spines used to assess endochondral ossification were decalcified and embedded in paraffin. Serial coronal sections were cut with a thickness of 5 μm and stained with Safranin O to identify areas undergoing chondrogenesis.

Statistical Analysis

Statistical analyses were performed using the StatView 5 program. All *p* values were calculated using ANOVA and Fisher's projected least significant difference (PLSD) significance test. A value of $p<0.05$ was considered significant.

Results

Oxy133 Induces Osteogenic Differentiation of Bone Marrow Stromal Cells, Embryonic Fibroblasts, and Human MSCs

To achieve the goal of developing a molecule capable of inducing osteogenic differentiation of osteoprogenitor cells, we modified the molecular structure of the most potent osteogenic naturally occurring oxysterol, 20S, based on our understanding of the structure activity relationships observed in over 100 previously synthesized analogues. We previously reported that robust osteogenic differentiation was achieved with two structural analogues of 20S, Oxy34 and Oxy49 (15). These molecules were formed by adding an α hydroxyl (OH) group on carbon 6 (C6) in both Oxy34 and 49, and a double bond between C25 and C27 in Oxy49 (Figure 1) (15). In studies reported here, we attempted to further improve on these two molecules by developing a more easily synthesized and more potent analogue that would be suitable for scale up into large amounts for future preclinical and clinical studies in large animals and humans, respectively. Through structure activity relationship studies a novel analogue, Oxy133, was synthesized according to the protocol described in Supplemental Materials (Chemical Synthesis and Characterization of Oxy133) and tested for osteoinductive activity. Oxy133 differs from Oxy34 and Oxy49 by the deletion of C27 and increasing the length of the side chain by one carbon (Figure 1). Importantly, Oxy133 can be more readily prepared on large scale due to inexpensive commercially available starting materials that result in a significantly less costly product compared to Oxy34 and Oxy49. Moreover, the alkyne addition used in the preparation of Oxy133 is superior to the Grignard chemistry used in the synthesis of Oxy34 and Oxy49 in terms of yield, purity of products (diastereoselectivity), and scalability. Further details about the synthesis of Oxy133 and its

distinct characteristics that make it more favorable as a potential drug candidate are described in Supplemental Material (Chemical Synthesis and Characterization of Oxy133).

Oxy133 was selected from several structural analogues of 20S because of its potency in inducing alkaline phosphatase (ALP) activity as measured by ALP enzymatic activity assay in C3H and M2 cells as we have previously reported for other oxysterol analogues (15). A dose-dependent increase in ALP activity was observed with Oxy133 at low micromolar (μM) concentrations (Figure 2A, B). The EC50 for Oxy133 was found to be approximately 0.5 μM in C3H (Figure 2A) and 0.44 μM in M2 cells (Figure 2B). The EC50 of Oxy34 and Oxy49 in C3H cells was found to be similar to what was previously reported in M2 cells, 0.8 and 0.9 μM, respectively, and significantly higher than the EC50 of Oxy133 (Figure 2A). Moreover, Oxy133 at high doses induced a greater level of ALP activity than similar doses of Oxy34 and Oxy49 in C3H cells (Figure 2A). It is also noteworthy that rhBMP2 at 200 ng/ml (a relatively high dose) induced ALP activity in cells to a similar degree to that induced by μM Oxy133 and two fold more than what was induced by 0.5 μM Oxy133 (Supplemental Figure 1)). Further effects of Oxy133 in inducing osteogenic differentiation of cells were confirmed through analysis of the expression of osteogenic differentiation marker genes Runx2, OSX, ALP, BSP, and OCN. Treatment with 2.5 μM Oxy133 induced Runx2 expression 2 and 3.2 fold after 4 and 7 days of treatment, respectively, which returned to baseline levels at 14 days (Figure 3A). OSX expression was significantly induced 3 fold after 2 days and remained elevated throughout the experiment reaching a maximum induction of 4.5 fold (Figure 3A). Treatment of cells with Oxy133 induced the expression of ALP 18 fold after 2 days which maximized to 120 fold after 4 days and then dropped to 22 fold after 7 and 14 days, respectively (Figure 3A). BSP expression was maximally induced 9 fold on day 4 and remained induced for the duration of the experiment in spite of lowering with the longer exposure of cells to Oxy133 (Figure 3A). Oxy133 treatment also induced the expression of osteoblast-specific gene, OCN, 2.8 fold after 4 days and reached a maximum of 4.2 fold after 14 days post-treatment (Figure 3A). Oxy133 induced robust matrix mineralization in cultures of C3H cells as determined by von Kossa staining (Figure 3B) and quantitative extracellular matrix ^{45}Ca incorporation assay after 21 days of treatment (Figure 3C). Comparison of Oxy133-induced osteogenic effects in parallel with those of Oxy34 and Oxy49 at EC50 of Oxy133 (for induction of ALP activity) showed significantly greater potency of Oxy133 in inducing ALP, OSX, and BSP mRNA expression after 4 days, OCN expression after 14 days, and ^{45}Ca incorporation after 21 days (Supplemental Figure 1). Furthermore, 200 ng/ml rhBMP-2 induced greater expression of ALP, OSX, and OCN but much lower expression of BSP than Oxy133 (Supplemental Figure 1). In addition, ^{45}Ca incorporation was induced significantly more by Oxy133 than that induced by 0.5 μM Oxy34, 0.5 μM Oxy49, or 200 ng/ml rhBMP-2 (Supplemental Figure 1). These data demonstrate the efficacy and potency of Oxy133 as an osteoinductive oxysterol.

The osteogenic effects of Oxy133 were also examined in primary human MSCs by assessing the expression of osteogenic genes 1 week, 2 weeks and 4 weeks post-treatment. ALP expression was high in untreated cells at all time points and there was no change with Oxy133 treatment (data not shown). After one week, a significant 2 fold increase in BSP expression was observed that was further increased to 4 fold after 2 and 4 weeks (Figure

3D). Oxy133 also resulted in a significant induction of OSX (3 fold) and OCN (2 fold) after 4 weeks (Figure 3D). Additionally, Oxy133 stimulated robust extracellular matrix mineralization in cultures of primary human MSCs as demonstrated by von Kossa staining after 5 weeks of treatment (Figure 3E).

Oxy133 Inhibits Adipogenic Differentiation of Embryonic Fibroblasts

In previous reports we had demonstrated the inhibitory effects of osteogenic oxysterols on adipogenic differentiation of multipotent mesenchymal cells, including C3H and M2 cells, and we had reported that this inhibitory effect was mediated through inhibition of PPARγ expression (14). We now report the anti-adipogenic effects of Oxy133 when applied to C3H cells treated with the PPARγ activator, troglitazone (Tro), to induce adipogenesis (Supplemental Figure 5). Oxy133 caused a significant inhibition of Tro-induced adipogenic differentiation marker genes PPARγ and aP2, as well as the formation of adipocytes as demonstrated by Q-RT-PCR and by Oil red O staining, respectively (Supplemental Figure 5).

Oxy133 Induces Osteogenic Differentiation Through Activation of Hh Pathway Signaling and Not Through BMP or Wnt Signaling

Prior research has demonstrated that 20S and its structural analogues Oxy34 and Oxy49 induce osteogenic differentiation via activation of Hh pathway signaling through binding to and allosteric activation of Smoothened (Smo) (15, 20, 26). However, the molecular mechanism for osteogenic oxysterol-mediated activation of Hh pathway signaling was not elucidated previously. Given its greater osteogenic activity, Oxy133 was a better tool for identifying the molecular mechanism by which Hh pathway activation and osteognesis are achieved by the semi-synthetic oxysterols. In order to confirm that Oxy133 also induces osteogenic differentiation through the Hh pathway, the effect of the selective Hh pathway inhibitor, cyclopamine, on Oxy133-induced ALP activity and expression of osteogenic differentiation markers ALP, BSP, and OSX was examined. Cyclopamine completely inhibited Oxy133-induced ALP activity and expression of osteogenic markers ALP, BSP, and OSX, in C3H cells (Figure 4A), as well as in M2 cells (data not shown) suggesting that Oxy133 also acts via the Hh signaling pathway. To further confirm the activation of Hh signaling by Oxy133, activation of a Gli-dependent luciferase reporter transfected into C3H cells was examined as we have previously reported (15,18). Oxy133 induced a dose-dependent increase in activity of the Gli-dependent reporter, reaching a 5 fold induction at 100 nM and a 17 fold induction at 1 μM Oxy133 (Figure 4B).

Furthermore, we examined the response of cells to Oxy133 in the presence of other Hh pathway activators, namely Shh, which activates the pathway by binding to Ptch and alleviating its inhibitory effect on Smo, and SAG, which directly binds to Smo. Treatment of cells for 3 days with a submaximal dose of Oxy133 (0.1 μM) together with submaximal doses of Shh (100 ng/ml) or SAG (10 μM) caused resulted in synergistic activation of Hh signaling measured by the induction of Ptch1, Gli1, and HIP (Supplemental Figure 7). Moreover, ALP mRNA expression and enzymatic activity were also synergistically induced by Oxy133 when added in the presence of Shh or SAG (Supplemental Figure 7).

In addition to examining the Hh pathway, we also assessed the potential role of the BMP/Smad pathway as well as Wnt signaling in mediating osteogenic responses to Oxy133. As expected, treatment of C3H cells with rhBMP-2 induced Smad activation as demonstrated by the increased levels of phosphorylated Smad (pSmad) after 15 and 30 minutes on Western blots (Supplemental Materials, Figure 2). Treatment of cells with Oxy133 did not increase pSmad levels in cells when treated for 15 or 30 minutes as well as after longer treatments for 24 and 48 hours (Supplemental Materials, Figure 1). Furthermore, Oxy133 treatment of did not induce the expression of BMP-2 or BMP-4 after 8, 24, or 48 hours as assessed by Q-RT-PCR (data not shown). In addition, treatment with BMP inhibitor, noggin (200 ng/ml), blocked rhBMP2-induced ALP activity in cells by >90% but only blocked Oxy133-induced ALP activity by <30% (Supplemental Materials, Figure 3). This effect of noggin is similar to what we previously reported for 20S and is likely due to inhibition of the synergy between baseline BMP/Smad activity present in cells with Oxy133-induced Hh signaling and osteogenesis (13, 27). Altogether, these data suggest that the BMP2/Smad pathway is not involved in Oxy133-induced osteogenesis.

We also examined the possible role of Wnt signaling in Oxy133-induced responses by treating C3H cells with the Wnt pathway inhibitor, Dkk-1. Dkk-1 (1 μg/ml) did not inhibit Oxy133-induced ALP activity (data not shown). Furthermore, we did not find any induction of the expression of Wnt signaling target genes Axin2, Nkd2, and Cyclin D1 in C3H cells treated for 48 hours with Oxy133, whereas lithium chloride, which is known to activate Wnt signaling, did induce the expression of Axin2 and Nkd2 but not Cyclin D1 (Supplemental Materials Figure 4). However, as previously shown for 20S, Oxy133 did induce the expression of Wnt target gene, Wif-1, which was completely blocked by the Hh pathway inhibitor, cyclopamine (Supplemental Figure 4), and therefore a Hh pathway mediated response.

Oxy133 Activates the Hedgehog Signaling Pathway by Binding to the Smoothened Receptor

We previously reported that 20S selectively activates Hh signaling by binding to the Smo receptor (20). To determine whether Oxy133 activates Hh signaling by the same mechanism, we tested the ability of Oxy133 to compete for YFP-tagged Smo (YFP-Smo) binding with a 20S analogue coupled to magnetic beads. As we previously reported, this analogue, nat-20S-yne, contains an alkyne moiety on the *iso*-octyl chain, allowing for click chemistry-mediated coupling to magnetic beads (20S-beads) (20). Using these beads for sterol-binding assays, the amount of YFP-Smo remaining on the beads relative to a no-competitor sample is measured by Western blotting. Compounds that bind Smo at the same site as 20S compete with the 20S-beads and reduce the amount of protein in the eluate. We have tested many other sterols both in Smo binding assays and Hh signaling assays and in all cases binding to Smo correlated with a change in Hh pathway activity (20). Both Oxy133 and 20S, the positive control, reduced the amount of YFP-Smo captured on 20S-coupled beads (Figure 4C). In an important control, a structurally related analogue, Oxy16, which cannot activate Hh signaling or osteogenesis (Parhami et al. unpublished observations) failed to prevent the interaction between YFP-Smo and 20S-beads (Figure 4C). This reduction in the amount of YFP-Smo captured by 20S-beads in the presence of free Oxy133

suggests that Oxy133 binds to the same site on Smo as 20S. It is important to emphasize that our assay is semi-quantitative and cannot be used to derive K_d for the interaction, principally because we do not know the concentration of YFP-Smo in the extract and the amount of 20S productively immobilized on beads.

Oxy 133 Stimulates Bone Formation and Spinal Fusion *In Vivo*

Eight week old Lewis rats were divided into five treatment groups that differed only by the reagent contained within the collagen sponge at the surgery site: Group 1-control vehicle (DMSO) only (n=7), Group II-5 μg rhBMP-2 (n=8), Group III-20 mg Oxy133 (n=7), Group IV-2 mg Oxy133 (n=8), and Group V-0.2 mg Oxy133 (n=8). Bone formation and spinal fusion were assessed at various time points post-operatively through radiographic analysis, and at sacrifice using manual assessment, μCT, and histology. Fusion rates at sacrifice are summarized in Figure 5.

Radiographic Analysis—The first sets of radiographs were performed four weeks after the operation. At this time point, bilateral fusion was observed in 8 of 8 animals in the rhBMP-2 group, 6 of 7 animals in the Oxy133-20 mg group, 3 of 8 animals in the Oxy133-2 mg group, and no fusion in the control and the Oxy133-0.2 mg groups. Unilateral fusion was observed in the remaining Oxy133-20 mg treated animal and in 3 animals treated with Oxy133-2 mg. This is in contrast to prior studies with Oxy34 and 49 in which no fusion was observed at the 4-week time point (15). By 6 weeks, all animals had fused bilaterally in the Oxy133-20 mg group. At 8 weeks, fusion was again noted in all animals in the rhBMP-2 and Oxy133-20 mg groups and in 4 of 8 of the Oxy133-2 mg group (Figure 5). No fusion mass was observed in the DMSO or Oxy133-0.2 mg (data not shown) groups in the final 8-week radiographs (Figure 5).

Manual Assessment and Gross Evaluation of Bone Formation—After sacrifice, the spines were explanted from each animal and subjected to manual assessment as we have previously described (15, 29-31). Gross evaluation and manual assessment results were similar to radiographic findings at 8 weeks. No unilateral or bilateral fusion was observed in the DMSO or Oxy133-0.2 mg groups. Some bone formation was noted in two animals in the Oxy133-0.2 mg group. Bilateral fusion was observed in all animals in the rhBMP-2 group and 6/7 animals in the Oxy133-20 mg group. The remaining animal in the Oxy 133-20 mg group had motion unilaterally despite significant bilateral fusion mass. Half (4/8) of the animals in the Oxy133-2 mg group had bilateral fusion confirmed on manual palpation while two additional animals had unilateral fusion and two animals had no evidence of fusion.

μCT and Histological Assessment—Assessment of bridging trabecular bone with μCT analysis confirmed results observed with radiographs, gross observation, and manual palpation (Figure 6). Although some bone formation was seen in 2 animals in the Oxy133-0.2 mg group, no bilateral fusions were observed in this group or the DMSO group. Bilateral bridging trabecular bone was seen in all animals in the rhBMP-2 group and the Oxy133-20 mg group. Bilateral fusion was also observed in 4 of 8 animals in the Oxy133-2 mg group with unilateral fusion in 2 additional animals. Fusion extending beyond the

intended level (L4-5) was observed in 6 animals in the rhBMP-2 group and in none of the Oxy133 animals. The results of the microstructural analysis from the μCT images are shown in the bottom panel of Figure 6. The total volume of the rhBMP-2 fusion masses was significantly greater than both the Oxy133-2 mg and 20-mg samples. However, the mean BV/TV ratio of the Oxy133-2 mg and 20-mg fusion masses was significantly greater than the rhBMP-2 group, indicating denser bone within the masses. Trabecular thickness did not significantly differ between rhBMP-2 and either Oxy133-2 mg or Oxy133-20 mg. Trabecular separation was significantly larger in the rhBMP-2 fusion masses compared to Oxy133-2 mg and Oxy133-20 mg, also indicating less density of bone in the rhBMP-2 fusion masses.

Histologic analysis was then performed in 2 representative animals in the DMSO group, rhBMP-2 group, Oxy133-20 mg group, and Oxy133-2 mg group. Histological assessment demonstrated the formation of trabecular bone within the fusion mass and continuous cortical bone connecting the transverse processes of the fully fused lumbar vertebrae in rats treated with rhBMP-2, or with the 2 or 20 mg dose of Oxy133 (Figure 7A). Bone formation was not present in specimens from control rats. The size of the fusion mass was increased in rats treated with rhBMP-2 compared to 20 mg or 2mg of Oxy133. However, visual inspection of the histological specimens indicated that rhBMP-2 also induced robust formation of adipocytes within the fusion mass, which was significantly less in groups treated with Oxy 133 (Figure 7B). In addition, visual inspection suggested that trabecular bone formation was more robust in the Oxy133-20 mg group compared with the rhBMP-2 group.

Oxy133 Stimulates Osteogenesis via Endochondral Ossification

An additional 16 rats underwent spine fusion as described earlier. Eight animals were treated with 20 mg of Oxy133 and 8 were treated with 5 μg of rhBMP-2, bilaterally. Two animals in each group were sacrificed at each time point: 1, 2, 4 and 8 weeks. In both the Oxy133 and rhBMP-2 groups, chondrogenesis was observed in the intertransverse process space at 1 week and appeared to be most robust at 2 weeks. At the 4-week and 8-week time points, the cartilage was almost entirely replaced by bone in the intertransverse process space in both groups (Figure 7C). Consistent with these in vivo findings, in vitro studies using a previously reported pellet culture of C3H cells that undergo chondrogenic differentiation after 2 weeks when treated with 10 ng/ml TGFβ3 (data not shown), showed that treatment of such cell pellets with 10 μM Oxy133 induces chondrogenic differentiation as determined by significant mRNA induction of chondrogenic differentiation marker genes aggrecan and collagen 10 after 14 days of treatment 5 and 4 fold, respectively (Supplemental Figure 6). Lower concentrations of Oxy133 did not induce the expression of these genes.

Discussion

Augmentation of bone growth and repair is of great clinical importance in fracture healing, spine fusion, osteoporosis and a number of other musculoskeletal disorders. The use of biologics is particularly helpful in certain clinical scenarios in which native bone growth is inadequate. This includes open fractures and fractures at high risk of non-union, and in

select patients undergoing spine fusion. Despite being initially approved for use in anterior lumbar interbody fusion, rhBMP-2 is now used off-label in posterior lumbar fusions as well as anterior and posterior cervical spine surgery (32-34). rhBMP-2 has been shown clinically to improve fusion rates when used in spine surgery; however, there is a significant financial cost associated with its use and there have been several reports regarding the safety concerns of rhBMP-2 (32). Most worrisome has been the soft tissue edema and inflammation associated with rhBMP-2 use in the cervical spine (35), which can lead to airway compromise and dysphagia (36). The quality and biomechanics of bone formed by rhBMP-2 is also of significant concern (37). Thus, developing a safe and effective alternative to current treatments would be of significant clinical value in treating orthopedic diseases requiring bone formation.

We previously reported that specific naturally occurring oxysterols as well as their semi-synthetic analogues have modest to potent osteogenic effects when used *in vitro* on osteoprogenitor cells and *in vivo* to induce spine fusion in rats (15). The present study identified Oxy133 as the most potent osteogenic and anti-adipogenic oxysterol with a synthesis route that is significantly more simple, efficient, and less costly than the synthetic route of other oxysterols, including Oxy34 and Oxy49, making it a realistic option for large scale, cost-effective production as a potential drug candidate. Additionally, markers of osteogenic differentiation were induced in human MSCs using Oxy133, suggesting that the osteogenic effects of Oxy133 demonstrated *in vitro* and in animal models *in vivo* are likely to be observed when applied clinically in humans. In our hands, different batches of primary human MSCs, all of which were purchased from Lonza, had different levels of responsiveness to osteogenic factors including rhBMP-2 and Oxy133 that is likely due to the heterogeneity in their degree of differentiation and multipotentiality. In this report and in our previous reports of the osteogenic effects of oxysterols, we have used cultures of undifferentiated mesenchymal cells that show robust responses to osteogenic oxysterols. However, it is noteworthy that in unpublished studies, we have found that robust osteogenic responses are also induced by Oxy133 in MC3T3-E1 calvarial preosteoblasts when treatment with Oxy133 is initiated after the cells have undergone osteogenic differentiation for 2 weeks in the presence of ascorbate and β-glycerophosphate. Therefore, the targets of Oxy133 in vivo are likely to be both undifferentiated as well as partially differentiated osteoblasts; this point will need to be directly verified in future studies.

As previously reported for other osteogenic oxysterols (15,18,20), Oxy133 induced osteogenesis through activation of the Hh signaling pathway by direct binding to the Smo receptor as evidenced by its ability to compete with 20S oxysterol for binding to Smo. In previous studies we had reported that 20S does not compete with cyclopamine, a selective antagonist of the Hh pathway that directly binds to Smo, and hence concluded that 20S and perhaps other osteogenic oxysterols do not activate Hh signaling through binding to Smo (18). However, given our present findings and those reported recently by other investigators (20, 26), it is likely that Oxy133 binds to Smo at a site distinct from the cyclopamine binding site and that allosteric activation of Hh signaling is indeed mediated through direct binding to Smo. Noteworthy are findings presented here that demonstrate synergistic activation of Hh signaling and osteogenic differentiation when cells are treated with Oxy133

together with either Shh or SAG. Shh activates the Hh pathway through binding to Ptch and alleviating its inhibitory effects on Smo. SAG directly binds to and activates Smo through a site different than the site to which oxysterols binds (26).

Importantly, Oxy133 did not induce the expression of BMP2, BMP4, or pSmad levels that would have hinted at a potential role of BMP signaling in Oxy133-induced osteogenesis. Similarly, Wnt signaling target gene expression was not induced by Oxy133 and Dkk-1 did not inhibit Oxy133-induced osteogenesis in C3H cells. In a previous study we reported that Dkk-1 inhibited 20S-induced osteogenesis in contrast to our findings here with Oxy133 (28). Although the reason for this difference between the naturally occurring oxysterol, 20S, and the oxysterol analogue, Oxy133, is not clear at this time, other differences have also been noted including activation of liver X receptor pathway by 20S but not by Oxy133 (Parhami and colleagues, unpublished observations). Taken together with the *in vivo* results demonstrating adipogenesis induced by rhBMP-2 but not by Oxy133 in the fusion mass, these findings suggest that Oxy133 promotes bone formation through a mechanism independent of BMP and Wnt signaling and thus may be less prone to the side effects and bone microstructure problems observed with rhBMP-2. In preliminary studies we have found that cyclopamine partially blocks the osteogenic responses to BMP2, consistent with previous reports by us and others showing synergistic induction of osteogenesis by Hh and Smad/BMP signaling (Supplemental Figure 8). Since we have not found any evidence of direct or indirect activation of Hh signaling by BMP2 *in vitro* evidenced by the absence of Shh or Ihh expression, Gli1 reporter activation, or Hh target gene expression (data not shown), and the presence of baseline Hh signaling when cells are cultured in the presence of FBS, inhibition of BMP2-induced osteogenic responses by cyclopamine is likely due to inhibition of synergy between BMP2 and baseline Hh signaling. Even though it appears that both BMP2 and Oxy133 induce spine fusion through endochondral ossification, their respective differential effects on cell signaling pathways most likely explains the adipogenic and inflammatory responses to BMP2 and not to Oxy133.

Although fusion rates with Oxy133 in this study were similar to those observed previously with Oxy34 and Oxy49, the time to fusion was quicker with Oxy133 as evidenced by bilateral fusion in over eighty percent of animals at four weeks in the Oxy133-20mg group. Bone formation was present at this time point with Oxy34 and Oxy49; however, no bilateral fusion had occurred. Interestingly, in our study, fusion rate and success were similar when rhBMP-2 or Oxy133-20mg was used. Moreover, consistent with prior studies of oxysterols and rhBMP-2, we observed a significant number of adipocytes histologically in the fusion mass of animals treated with rhBMP-2 compared to those treated with Oxy133 (15,37). Although the significance of adipogenesis induced by rhBMP-2 in the fusion mass is not clear, given the common osteoprogenitors that give rise to both osteoblasts and adipocytes, we speculate that adipogenesis occurs at the expense of bone formation, compromising the quality of the bone that is formed by rhBMP-2. Importantly, quantitative μCT analysis demonstrated a greater bone volume to tissue volume ratio in the Oxy133 fusion masses and less trabecular separation when compared to rhBMP-2. These findings support our qualitative analysis of the bone histology in which an abundance of adipose tissue was observed in the fusion masses formed by rhBMP-2. In addition, we found no evidence of

heterotopic ossification in the Oxy133 treated spines, with the fusion masses confined to the L4-5 intertransverse process space. In contrast, fusion beyond the intended level often occurred in rhBMP-2 treated animals. Moreover, although Oxy133 induced bone formation via endochondral osteogenesis, in separate unpublished studies we have found that Oxy133 also stimulates bone formation during repair of cranial defects in rabbits, and hence stimulates repair even in bones that form through intramembranous osteogenesis.

In summary, Oxy133 stimulates bone formation by direct binding to Smo and subsequent activation of Hh signaling, resulting in osteogensis via endochondral ossification and bone formation with similar fusion rates and improved microstructural properties when compared to rhBMP-2. As such, we propose that Oxy 133 is a suitable candidate for further preclinical and clinical development as an osteoinductive therapy for stimulation of localized bone formation in spine fusion, fracture repair, and a number of additional clinical applications.

Supplementary Material

Refer to Web version on PubMed Central for supplementary material.

Acknowledgments

Studies reported here were supported by the NIH/NIAMS grant RO1AR059794. We are grateful to Kamran Movassaghi, Saeedeh Shapourifar-Tehrani, and Voicu Ciobanu for technical assistance.

References

1. Johnson EE, Urist MR. Human bone morphogenetic protein allografting for reconstruction of femoral nonunion. Clin Orthop Relat Res. 2000; 371:61–74. [PubMed: 10693551]
2. Mundy GR. Directions of drug discovery in osteoporosis. Annu Rev Med. 2002; 53:337–54. [PubMed: 11818478]
3. Rodan GA, Martin TJ. Therapeutic Approaches to Bone Diseases. Science. 2000; 289:1508–14. [PubMed: 10968781]
4. Yoon ST, Boden SD. Osteoinductive molecules in orthopaedics: basic science and preclinical studies. Clin Orthop Relat Res. 2002; 395:33–43. [PubMed: 11937864]
5. Arrington ED, Smith WJ, Chambers HG, Bucknell AL, Davino NA. Complications of iliac crest bone graft harvesting. Clin Orthop Relat Res. 1996; 329:300–9. [PubMed: 8769465]
6. Vaccaro AR, Chiba K, Heller JG, Patel TC, Thalgott JS, Truumees E, Fischgrund JS, Craig MR, Berta SC, Wang JC. Bone grafting alternatives in spinal surgery. Spine J. 2002; 2:206–15. [PubMed: 14589495]
7. Rihn JA, Kirkpatrick K, Albert TJ. Graft options in posterolateral and posterior interbody lumbar fusion. Spine. 2010; 35:1629–39. [PubMed: 20628336]
8. Mitka M. Questions about spine fusion product prompt a new process for reviewing data. JAMA. 2011; 306:1311–2. [PubMed: 21954470]
9. Lewandrowski KU, Nanson C, Calderon R. Vertebral osteolysis after posterior interbody lumbar fusion with recombinant human bone morphogenetic protein 2: a report of five cases. Spine J. 2007; 7:609–14. [PubMed: 17526434]
10. Wong DA, Kumar A, Jatana S, Ghiselli G, Wong K. Neurologic impairment from ectopic bone in the lumbar canal: a potential complication of off-label PLIF/TLIF use of bone morphogenetic protein-2 (BMP-2). Spine J. 2008; 8:1011–8. [PubMed: 18037352]
11. Smucker JD, Rhee JM, Singh K, Yoon ST, Heller JG. Increased swelling complications associated with off-label usage of rhBMP-2 in the anterior cervical spine. Spine. 2006; 31:2813–9. [PubMed: 17108835]

12. Carragee EJ, Hurwitz EL, Weiner BK. A critical review of recombinant human bone morphogenetic protein-2 trials in spinal surgery: emerging safety concerns and lessons learned. Spine J. 2011; 11:471–91. [PubMed: 21729796]
13. Kha HT, Basseri B, Shouhed D, Richardson J, Tetradis S, Hahn TJ, Parhami F. Oxysterols regulate differentiation of mesenchymal stem cells: pro-bone and anti-fat. J Bone Miner Res. 2004; 19:830–40. [PubMed: 15068507]
14. Kim WK, Meliton V, Amantea CM, Hahn TJ, Parhami F. 20(*S*)-hydroxycholesterol inhibits PPARgamma expression and adipogenic differentiation of bone marrow stromal cells through a Hedgehog-dependent mechanism. J Bone Miner Res. 2007; 22:1711–9. [PubMed: 17638575]
15. Johnson JS, Meliton V, Kim WK, Lee KB, Wang JC, Nguyen K, Yoo D, Jung ME, Atti E, Tetradis S, Pereira RC, Magyar C, Nargizyan T, Hahn TJ, Farouz F, Thies S, Parhami F. Novel oxysterols have pro-osteogenic and anti-adipogenic effects in vitro and induce spinal fusion in vivo. J Cell Biochem. 2011; 112:1673–84. [PubMed: 21503957]
16. Zhao L, Li G, Chan K, Wang Y, Tan P. Comparison of multipotent differentiation potentials of murine primary bone marrow stromal cells and mesenchymal stem cell line C3H10T1/2. Calcif Tissue Int. 2009; 84:56–64. [PubMed: 19052794]
17. Parhami F, Morrow AD, Balucan J, Leitinger N, Watson AD, Tintut Y, Berliner JA, Demer LL. Lipid oxidation products have opposite effects on calcifying vascular cell and bone cell differentiation. A possible explanation for the paradox of arterial calcification in osteoporotic patients. Arterioscler Thromb Vasc Biol. 1997; 17:680–7. [PubMed: 9108780]
18. Dwyer JR, Sever N, Carlson M, Nelson SF, Beachy PA, Parhami F. Oxysterols are novel activators of the Hedgehog signaling pathway in pluripotent mesenchymal cells. J Biol Chem. 2007; 282:8959–68. [PubMed: 17200122]
19. Kim WK, Meliton V, Bourquard N, Hahn TJ, Parhami F. Hedgehog signaling and osteogenic differentiation in multipotent bone marrow stromal cells are inhibited by oxidative stress. J Cell Biochem. 2010; 111:1199–209. [PubMed: 20717924]
20. Nachtergaele S, Mydock LK, Krishnan K, Rammohan J, Schlesinger PH, Covey DF, Rohatgi R. Oxysterols are allosteric activators of the oncoprotein Smoothened. Nat Chem Biol. 2012; 8:211–20. [PubMed: 22231273]
21. Rohatgi R, Milenkovic L, Corcoran RB, Scott MP. Hedgehog signal transduction by Smoothened: pharmacologic evidence for a 2-step activation process. Proc Natl Acad Sci USA. 2009; 106:3196–201. [PubMed: 19218434]
22. Alanay A, Chen C, Lee S, Murray SS, Brochmann EJ, Miyazaki M, Napoli A, Wang JC. The adjunctive effect of a binding peptide on bone morphogenetic protein enhanced bone healing in a rodent model of spinal fusion. Spine. 2008; 33:1709–13. [PubMed: 18580546]
23. Miyazaki M, Sugiyama O, Tow B, Zou J, Morishita Y, Wei F, Napoli A, Sintuu C, Lieberman JR, Wang JC. The effects of lentiviral gene therapy with bone morphogenetic protein-2-producing bone marrow cells on spinal fusion in rats. J Spinal Disord Tech. 2008; 21:372–9. [PubMed: 18600149]
24. Pereira RC, Stadmeyer LE, Smith DL, Rydziel S, Canalis E. CCAAT/Enhancer-binding protein homologous protein (CHOP) decreases bone formation and causes osteopenia. Bone. 2007; 40:619–26. [PubMed: 17095306]
25. Magyar CE, Aghaloo TL, Atti E, Tetradis S. Ostene, a new alkylene oxide copolymer bone hemostatic material, does not inhibit bone healing. Neurosurgery. 2008; 63:373–378. discussion 378. [PubMed: 18981846]
26. Nedelcu D, Liu J, Xu Y, Jao C, Salic A. Oxysterol binding to the extracellular domain of Smoothened in Hedgehog signaling. Nature Chem Bio. 2013 Published Online: July 7.
27. Richardson JA, Amantea CM, Kianmahd B, Tetradis S, Lieberman JR, Hahn TJ, Parhami F. Oxysterol-induced osteoblastic differentiation of pluripotent mesenchymal cells is mediated through a PKC- and PKA-dependent pathway. J Cell Biochem. 2007; 100:1131–1145. [PubMed: 17031848]
28. Amantea CM, Kim WK, Meliton V, Tetradis S, Parhami F. Oxysterol-induced osteogenic differentiation of marrow stromal cells is regulated by Dkk-1 inhibitable and PI3-kinase mediated signaling. J Cell Biochem. 2008; 105:424–436. [PubMed: 18613030]

29. Sintuu C, Simon RJ, Miyazaki M, Morishita Y, Hymanson HJ, Taghavi C, Brochmann EJ, Murray SS, Wang JC. Full-length spp24, but not its 18.5-kDa proteolytic fragment, inhibits bone-healing in a rodent model of spine fusion. J Bone Joint Surg Am. 2011; 93:1022–32. [PubMed: 21655895]

30. Miyazaki M, Morishita Y, He W, Hu M, Sintuu C, Hymanson HJ, Falakassa J, Tsumura H, Wang JC. A porcine collagen-derived matrix as a carrier for recombinant human bone morphogenetic protein-2 enhances spinal fusion in rats. Spine J. 2009; 9:22–30. [PubMed: 18805060]

31. Zhu W, Rawlins BA, Boachie-Adjei O, Myers ER, Arimizu J, Choi E, Lieberman JR, Crystal RG, Hidaka C. Combined bone morphogenetic protein-2 and -7 gene transfer enhances osteoblastic differentiation and spine fusion in a rodent model. J Bone Miner Res. 2004; 19:2021–32. [PubMed: 15537446]

32. Shields LBE, Raque GH, Glassman SD, Campbell M, Vitaz T, Harpring J, Shields CB. Adverse effects associated with high-dose recombinant human bone morphogenetic protein-2 use in anterior cervical spine fusion. Spine. 2006; 31:542–7. [PubMed: 16508549]

33. Baskin DS, Ryan P, Sonntag V, Westmark R, Widmayer MA. A prospective, randomized, controlled cervical fusion study using recombinant human bone morphogenetic protein-2 with the CORNERSTONE-SR allograft ring and the ATLANTIS anterior cervical plate. Spine. 2003; 28:1219–1224. [PubMed: 12811263]

34. Robin BN, Chaput CD, Zeitouni S, Rahm MD, Zerris VA, Sampson HW. Cytokine-mediated inflammatory reaction following posterior cervical decompression and fusion associated with recombinant human bone morphogenetic protein-2: a case study. Spine. 2010; 35:E1350–1354. [PubMed: 20938385]

35. Garrett MP, Kakarla UK, Porter RW, Sonntag VKH. Formation of painful seroma and edema after the use of recombinant human bone morphogenetic protein-2 in posterolateral lumbar spine fusions. Neurosurgery. 2010; 66:1044–1049. [PubMed: 20495420]

36. Stachniak JB, Diebner JD, Brunk ES, Speed SM. Analysis of prevertebral soft-tissue swelling and dysphagia in multilevel anterior cervical discectomy and fusion with recombinant human bone morphogenetic protein-2 in patients at risk for pseudarthrosis. J Neurosurg Spine. 2011; 14:244–9. [PubMed: 21184639]

37. Zara JN, Siu RK, Zhang X, Shen J, Ngo R, Lee M, Li W, Chiang M, Chung J, Kwak J, Wu BM, Ting K, Soo C. High doses of bone morphogenetic protein 2 induce structurally abnormal bone and inflammation in vivo. Tissue Eng Part A. 2011; 17:1389–99. [PubMed: 21247344]

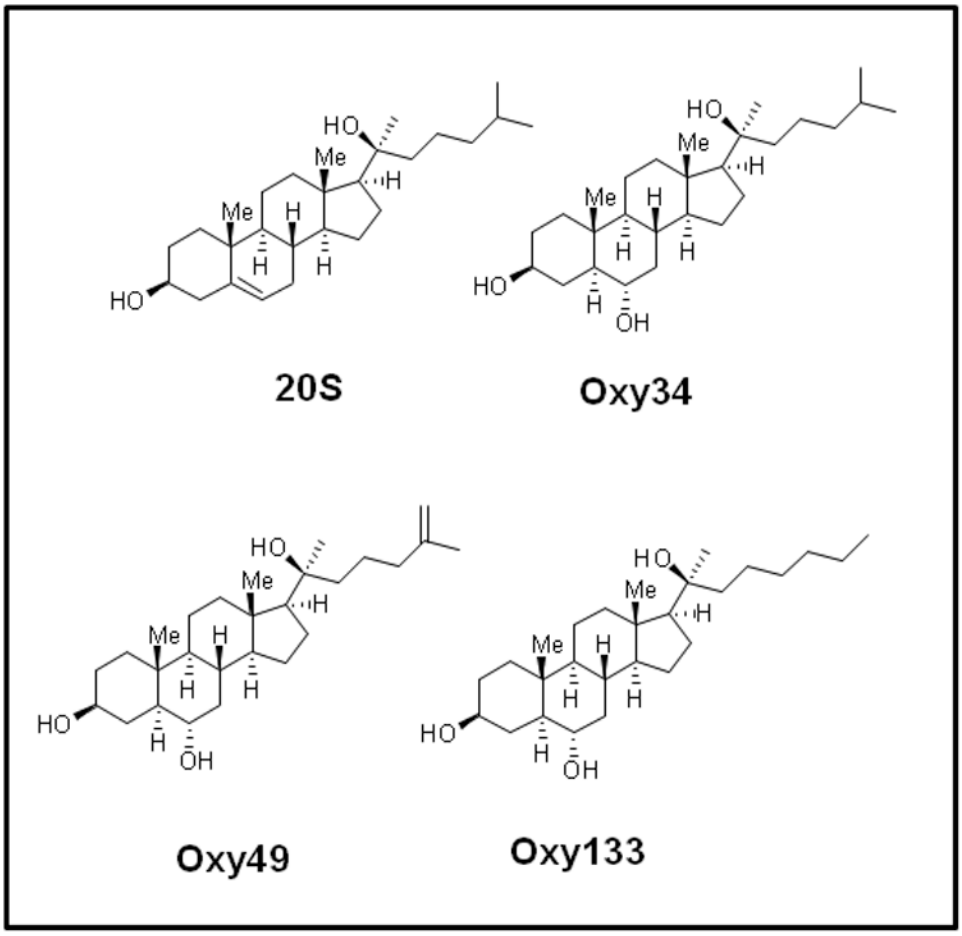

Figure 1. Molecular structures of osteogenic oxysterols

The molecular structures of 20(*S*)-hydroxycholesterol (20S), Oxy34, Oxy49, and Oxy133 are shown. Oxy34 is different from 20S in having an extra OH group on C6 and the double bond between C5 and C6 is eliminated. Oxy49 has a similar structure to Oxy34 and includes a double bond between C25 and C27. Oxy133 differs from Oxy34 and 49 by the deletion of C27 and increasing the length of the side chain by one carbon.

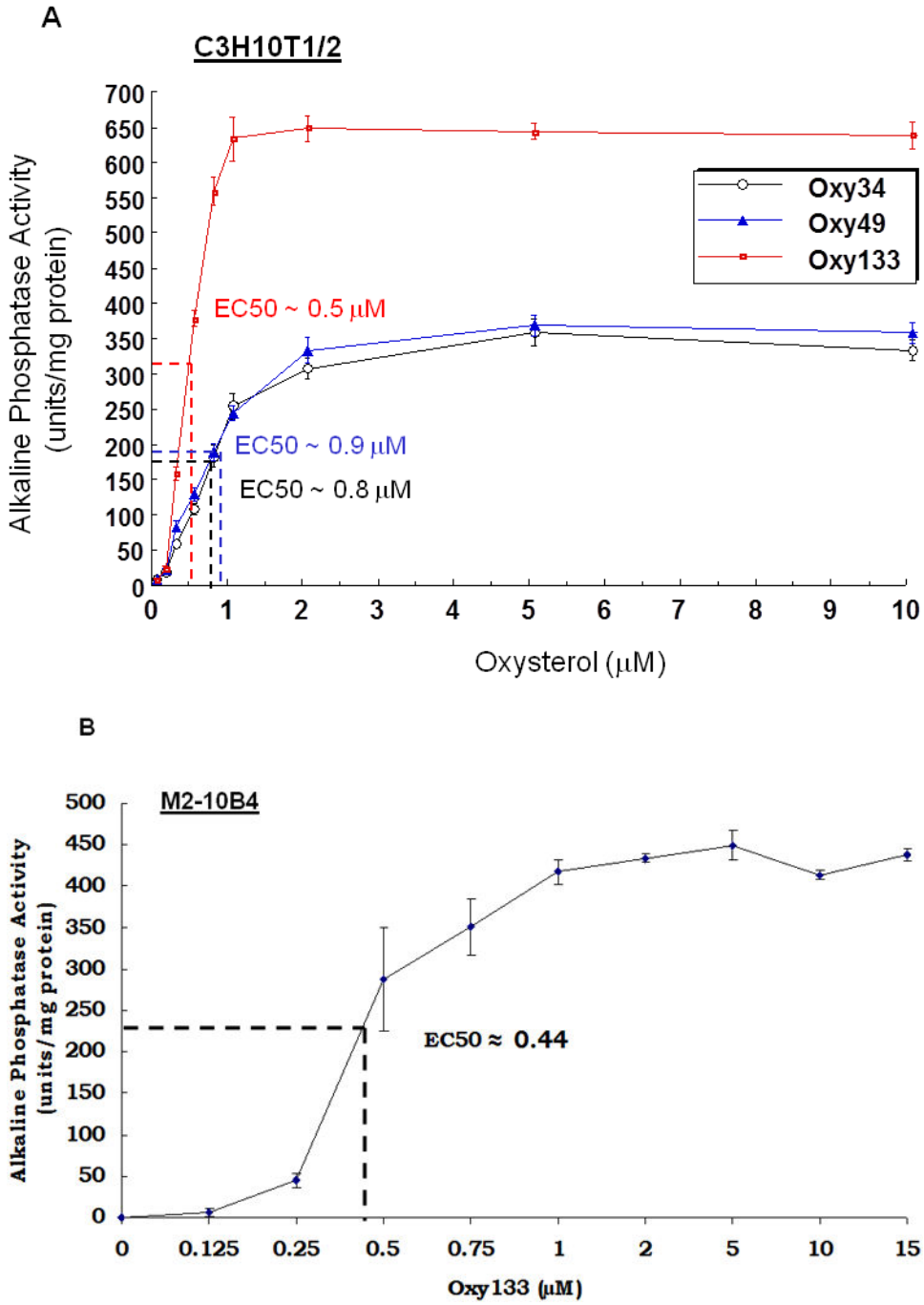

Figure 2. Dose-dependent activation of alkaline phosphatase activity by oxysterols

(A) C3HT101/2 cells or **(B)** M2-10B4 cells at confluence were treated with control vehicle or 0.125-10 μM of Oxy133. For direct comparison to Oxy133, C3H cells were also treated with Oxy34 and Oxy49 (A). After 4 days, alkaline phosphatase (ALP) activity was measured in whole cell extracts. Data from a representative of three separate experiments are reported as the mean of triplicate determinations ± SD and normalized to protein concentration. (p <0.0001 for cells treated with 0.25 μM or higher dose of all oxysterols vs. control vehicle treated cells).

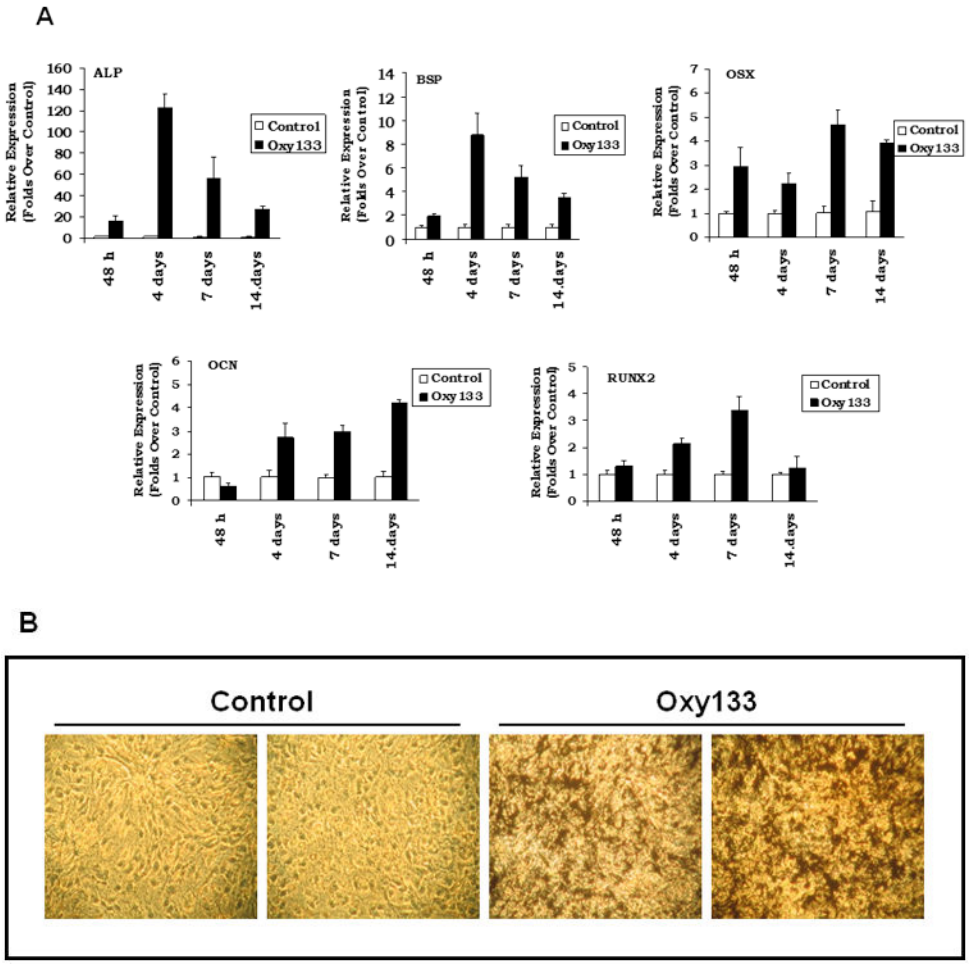

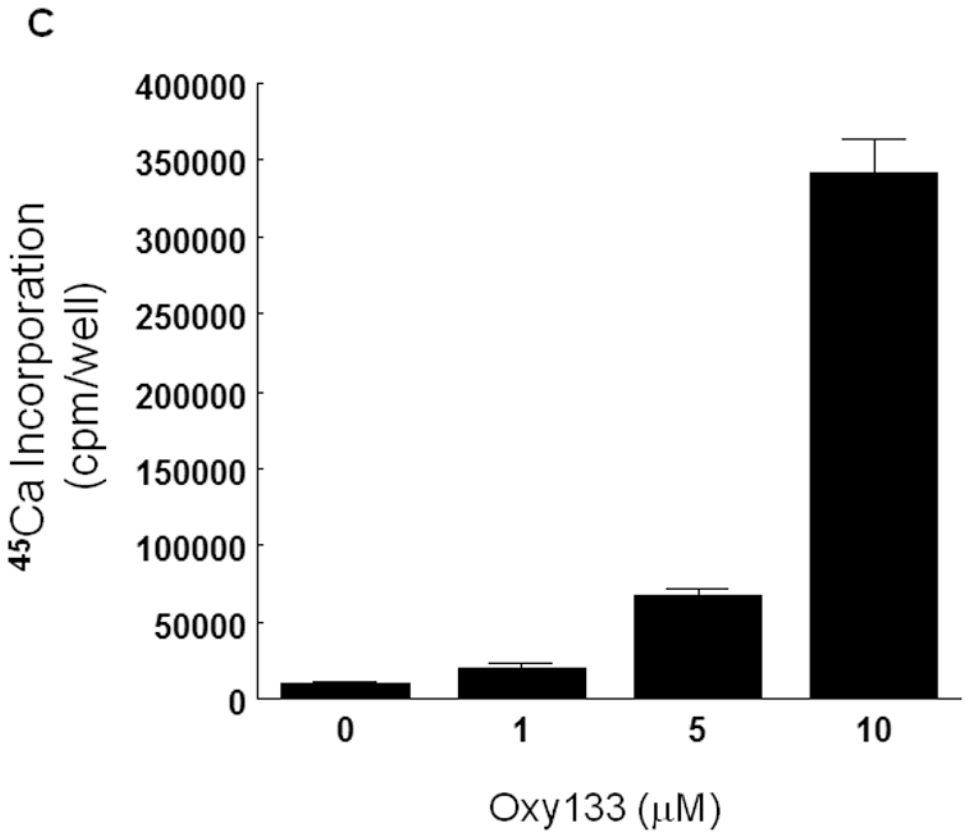

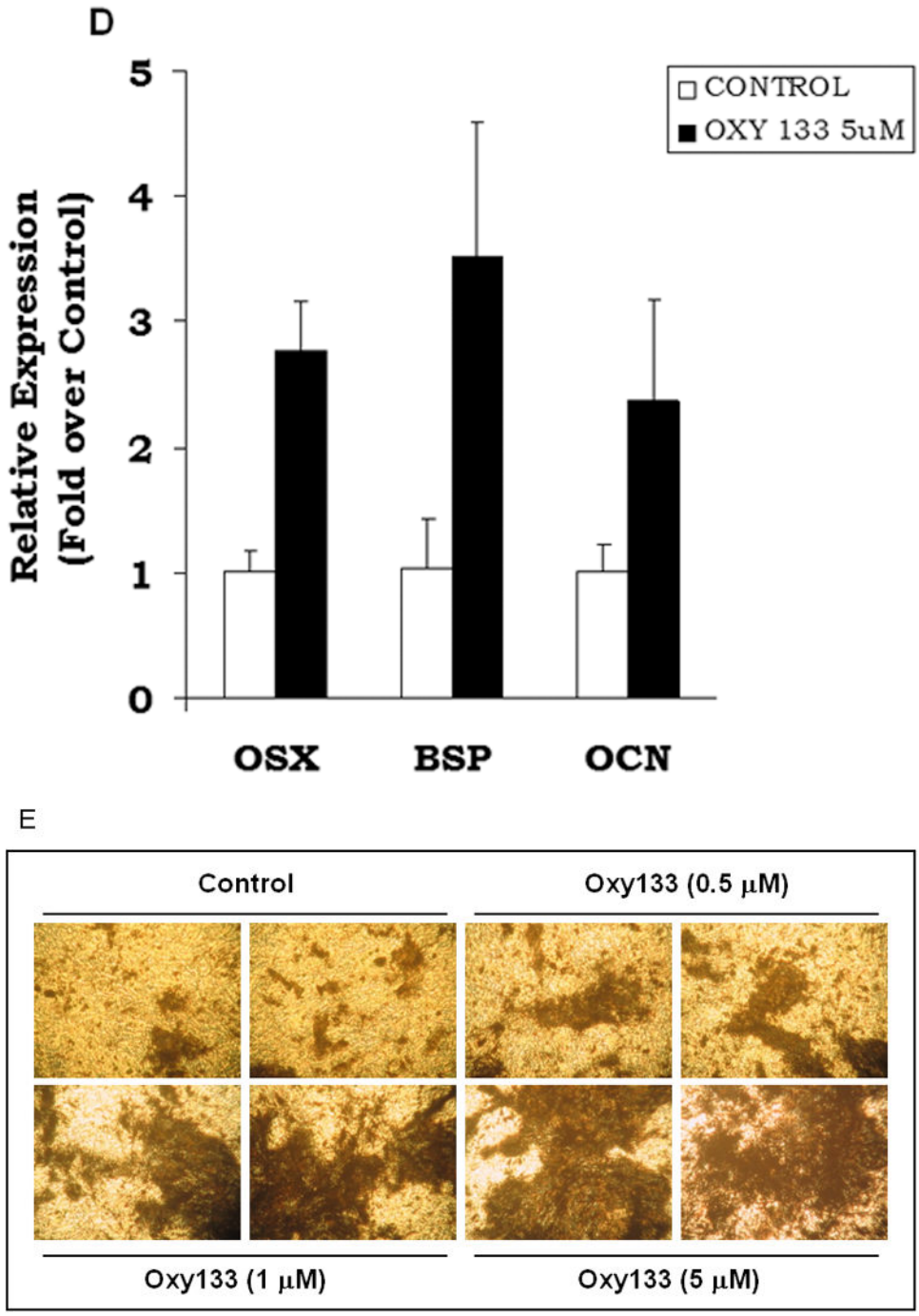

Figure 3. Oxy133 induces osteogenic differentiation

(A) C3HT101/2 cells at confluence were treated with control vehicle or 2.5 μM Oxy133 in osteogenic media. Expression of osteogenic genes Runx2, ALP, BSP, OSX, and OCN was measured by quantitative real-time PCR after 48 hours (48h), 4, 7, and 14 days of treatment. Results from a representative experiment are reported as the mean of triplicate determinations ± SD. (p<0.005 for control vs. Oxy133 at all time points for ALP, BSP and OSX and at 4, 7, and 14 days for Runx2 and OCN). **(B)** C3H10T1/2 cells were treated with

control vehicle or 2.5 μM Oxy133 for 3 weeks. To examine extracellular mineralization von Kossa staining was performed and mineralized matrix appears as dark black staining under light microscopy (10×). **(C)** In parallel cultures to those described in (B), mineralization was quantified using a ^{45}Ca incorporation assay ($p<0.005$ for control vs. all concentrations of Oxy133). **(D)** Primary human MSCs were treated in osteogenic medium with control vehicle or 5 μM Oxy133 for 4 weeks. Expression of osteogenic genes OSX, BSP, and OCN was measured by quantitative real-time PCR. Results from a representative experiment are reported as the mean of triplicate determination ± SD ($p<0.05$ for all genes in control vs. Oxy133 treated cells). **(E)** Primary human MSCs were treated in osteogenic medium with control vehicle or 0.5, 1, and 5 μM Oxy133 for 5 weeks. To examine extracellular mineralization von Kossa staining was performed and mineralized matrix appears as dark black staining under light microscopy (10×).

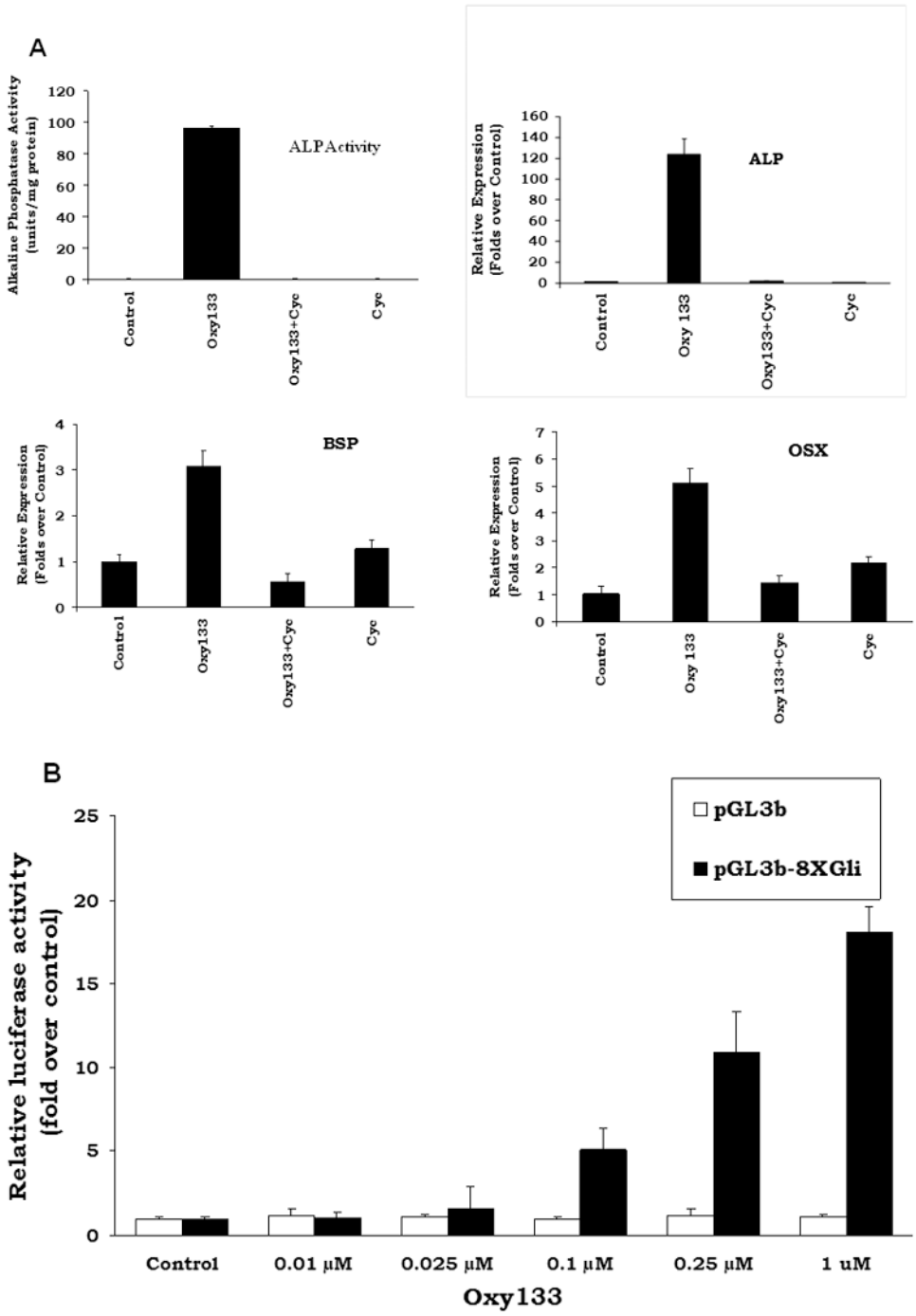

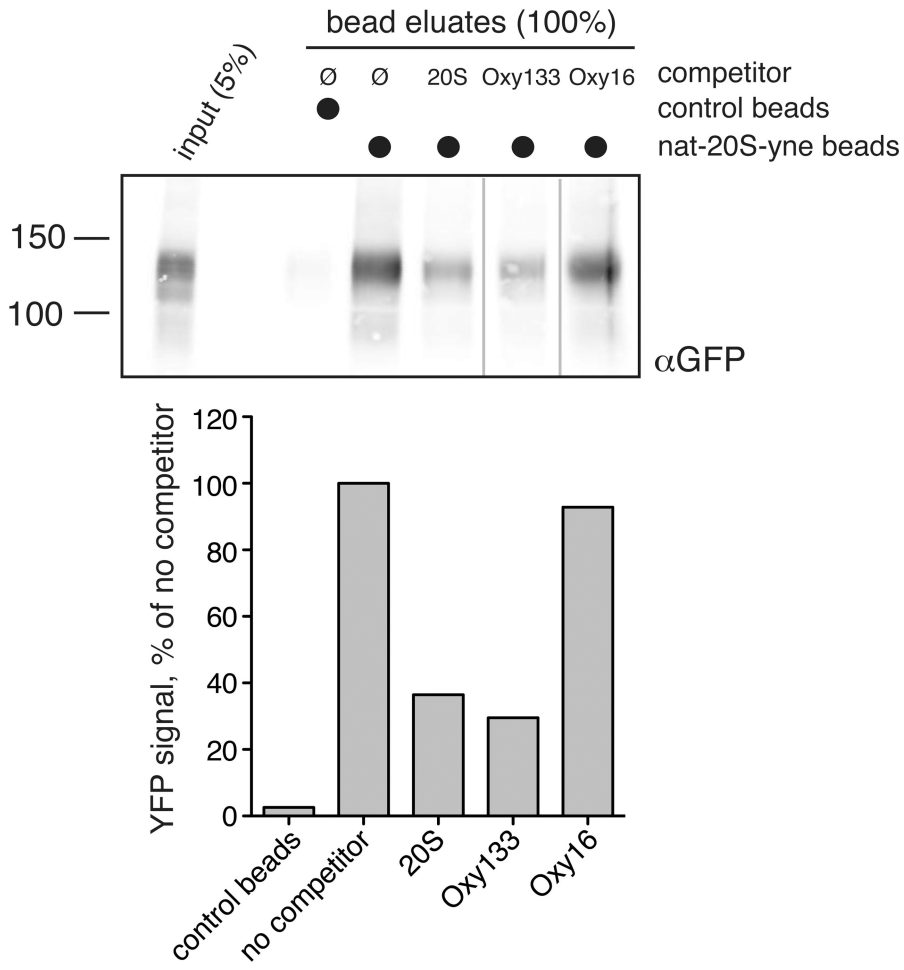

Figure 4. The role of Hedgehog pathway in Oxy133-induced osteogenic differentiation

(A) C3H10T1/2 cells at confluence were treated in osteogenic medium with control vehicle or Oxy133 in the presence or absence of 4 μM cyclopamine (Cyc). After 4 days ALP activity, and after 7 days the expression of osteogenic genes ALP, BSP, and OSX was measured by quantitative real-time PCR ($p<0.001$ for control vs. Oxy133, and for Oxy133 vs. Oxy133+Cyc for ALP activity and for the expression of all genes shown). **(B)** C3H10T1/2 cells were transfected with control plasmid (pGL3b) or a plasmid containing 8×-Gli luciferase reporter and treated with control vehicle or Oxy133, and luciferase activity was determined after 48 hours. Results from a representative experiment are reported as the mean of triplicate determinations ± SD. ($p<0.001$ for control vs. Oxy133 at 100 nM, 250 nM, and 1 μM Oxy133). **(C)** The amount of YFP-Smo captured by 20S beads or control beads was compared in samples containing either no competitor or 50μM of a free competitor sterol (20S, Oxy133 or Oxy16). The YFP-Smo captured by the beads was measured by Western blot (top) and plotted (bottom) relative to the amount captured in the binding reaction with no competitor.

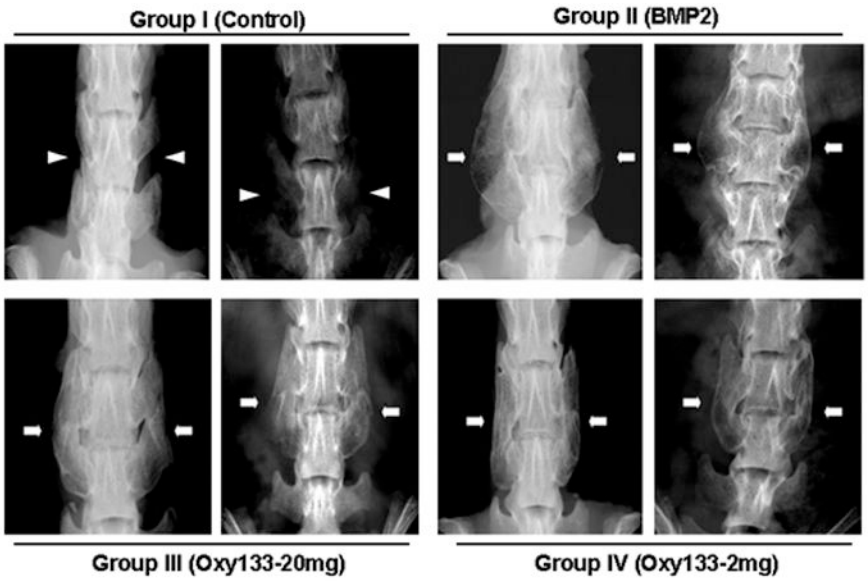

	X-ray (%)	Micro-CT (%)	Manual Palpation (%)
Control	0	0	0
BMP2	100	100	100
Oxy133 20 mg	100	100	86
Oxy133 2 mg	50	50	50
Oxy133 0.2 mg	0	0	0

Figure 5. Plain radiographs of fusion masses and fusion rates in animals treated with rhBMP-2 and Oxy133

Top panel: Faxitron images of two representative animals from the indicated groups at 8 weeks postoperatively are shown. Arrowheads signify lack of bone formation; arrows signify bone formation. Group I (Control); intertransverse process space with no bone formation. Group II (BMP2); bridging bone mass and bilateral fusion at L4–L5. Group III (Oxy133–20 mg); bridging bone mass and bilateral fusion at L4–L5. Group IV (Oxy133–2mg); bridging bone mass and bilateral fusion at L4–L5 in animals that showed induction of fusion by Oxy133. Bottom panel: fusion rates in animals treated with control, rh-BMP2 or Oxy133 as assessed by xrays, μCT, and manual palpation.

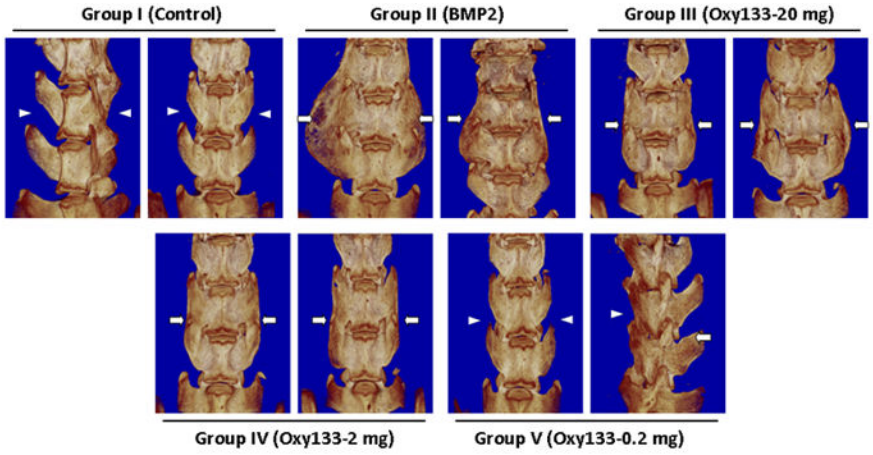

	Fusion Mass Total Tissue Volume (mm^3)	Fusion Mass Bone Volume (mm^3)	Fusion Mass Bone Volume to Tissue Volume (%)	Fusion Mass Trabecular Thickness (μm)	Fusion Mass Trabecular Separation (μm)
BMP2 5 μg	106.909*	20.126	19.633*	131.131	446.126*
Oxy133 2mg	78.586	21.217	27.104	134.008	321.693
Oxy133 20mg	79.934	19.592	24.565	124.737	310.912

* indicates statistically significant difference ($p<0.01$) in total tissue volume, bone volume to tissue volume ratio, and trabecular separation between BMP2 and Oxy133 20mg and 2mg. No differences were observed in bone volume or trabecular thickness.

Figure 6. μCT images and quantification of bone microstructure of fusion masses formed by rhBMP-2 and Oxy133

. Top panel: μCTs of two representative animals from the indicated groups are shown. Arrowheads signify lack of bone formation; arrows signify bone formation. Group I (Control); intertranverse process space with no bone formation. Group II (BMP2); bone mass bridging the intertransverse process space and bilateral fusion at L4–L5. Group III (Oxy133–20mg); bone mass bridging the intertransverse process space and bilateral fusion at L4–L5. Group IV (Oxy133–2mg); bone mass bridging the intertransverse process space and bilateral fusion at L4–L5 in animals that showed induction of fusion by Oxy133. Group V (Oxy133–0.2mg); arrow on the far right indicates a small amount of bone formation from the L5 transverse process. Bottom panel: Quantitative assessment of bone microstructure from μCT imaging.

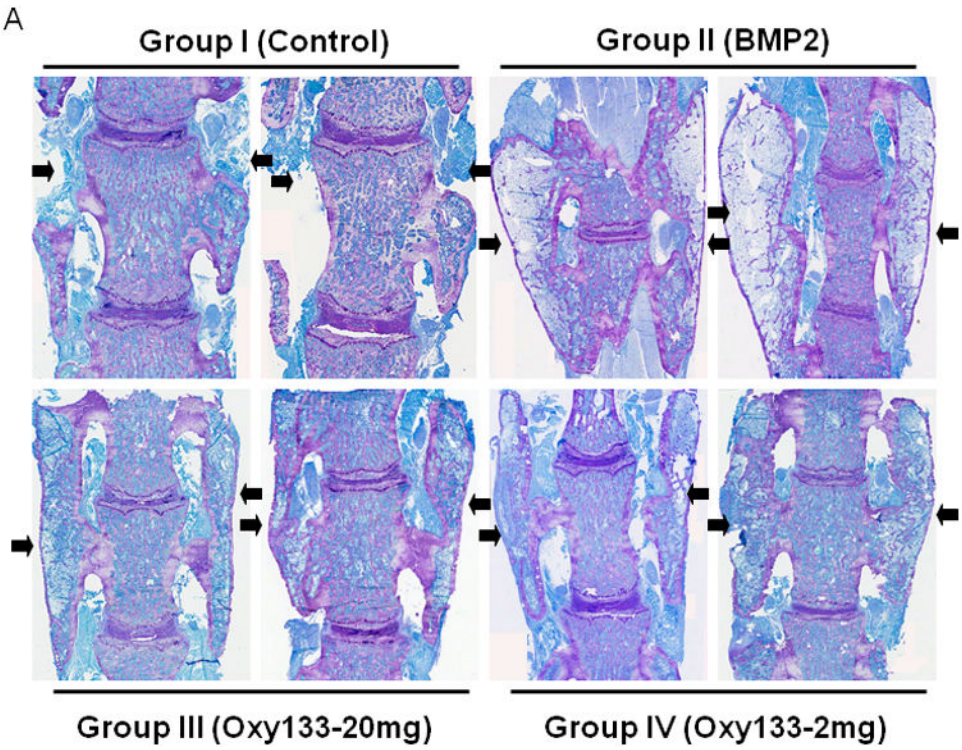

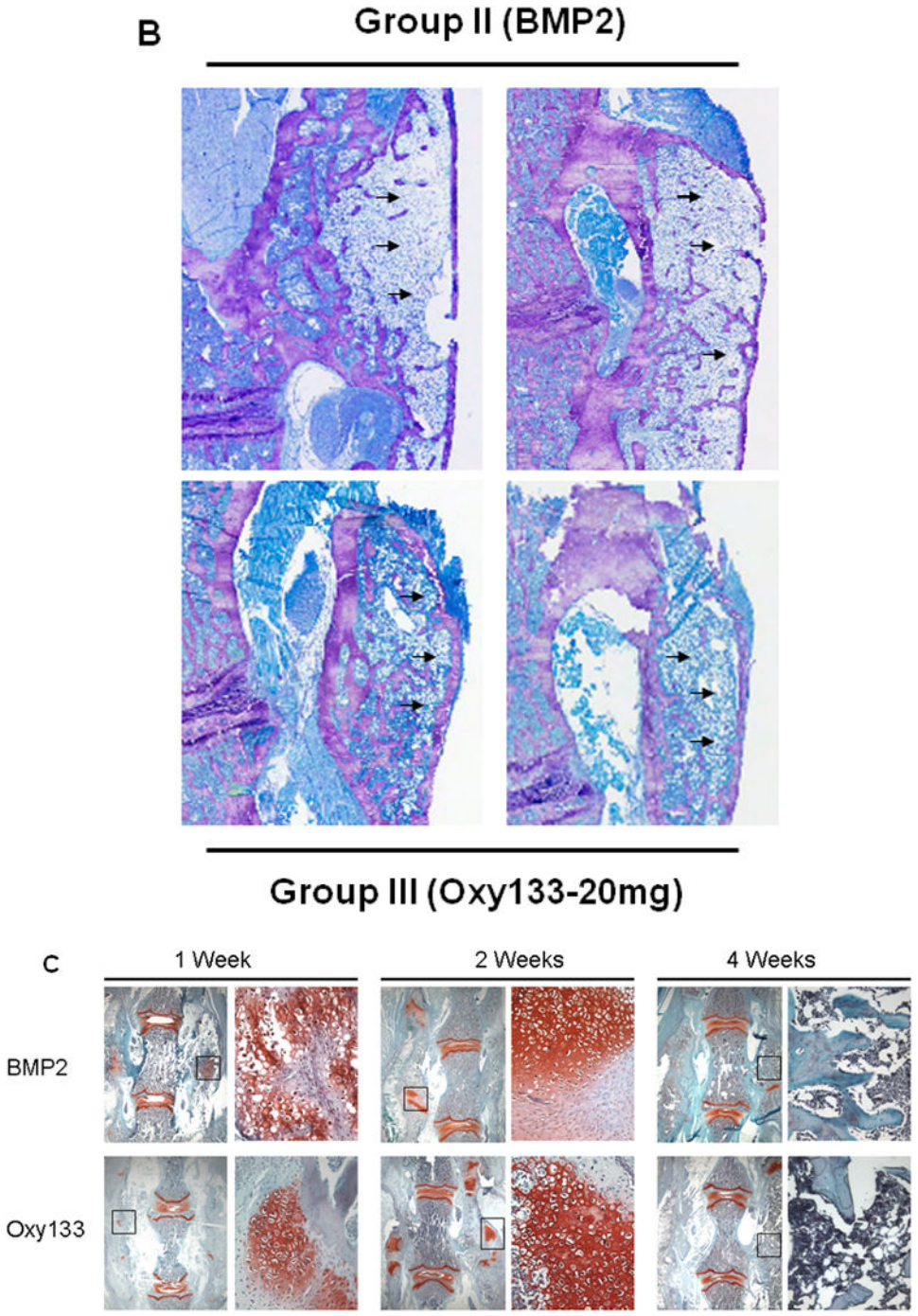

Figure 7. Histological analysis of the effect of Oxy133 on spinal fusion

(A) Coronal histological sections of two separate representative animals from each group are shown (10×). Group I (Control) has no significant bone formation at the intertransverse process space (arrowheads). Group II (BMP2) demonstrates bridging bone at L4–L5 (arrows) with clear evidence of trabecular and cortical bone forming the fusion mass. Group III (Oxy133–20mg) and Group IV (Oxy133–2 mg) specimens demonstrate significant bone formation at the intertransverse process space (arrows) with trabecular and cortical bone

formation comparable to that induced by BMP2. **(B)** Coronal histological sections from two animals each in Groups II (BMP2) and Group III (Oxy133–20 mg) demonstrate significant adipocyte formation in the fusion mass of BMP2 treated animals and substantially fewer adipocytes in the fusion mass from oxysterol treated animals (arrows, magnification 20×). **(C)** Coronal Safranin O stained sections of animals treated with Oxy133 and rhBMP-2 at 1, 2 and 4 weeks. Areas stained red indicate sites of chondrogenesis. At each time point, the image on the left is low magnification (7×). The region outlined in the low magnification image is shown to the right at high magnification (200×), demonstrating cartilage in the intertransverse process sapce at 1 and 2 weeks, which has been replaced by bone at 4 weeks.